Supporting Information

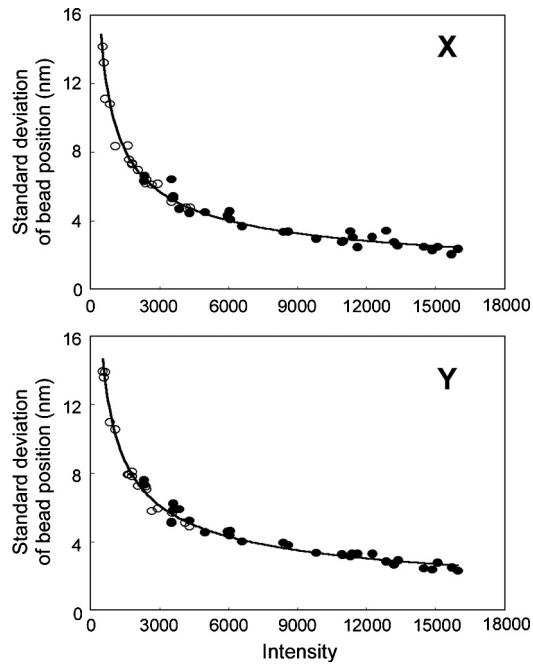## Nakamura et al. 10.1073/pnas.1007448107

Fig. S1. Standard deviations of the X and Y positions as a function of fluorescence intensity of 100 nm-fluorescent beads that are firmly attached onto a cover slip. The positions of the beads were determined from images recorded by the EMCCD camera at 0.4 msec intervals. Open and closed circles are the data obtained by an ultra-high-pressure mercury lamp and a dye laser, respectively. Note that the theoretical curves in solid lines are well fitted to the data points.

Fig. S2. Rotational fluctuations of 100 nm-fluorescent beads firmly attached onto a cover slip (*A*, *B*) or those attached to the sticky flagellar filaments of the *motA-motB* double null mutant (*C*, *D*). Bead images were recorded by the EMCCD camera at 0.4 msec intervals. Standard deviations of bead angles are (*A*) 0.78°, (*B*) 0.97°, (*C*) 2.3°, and (*D*) 2.6° by assuming the radius of rotation of the bead to be *ca*. 230 nm.

Fig. S3. Dominant negative effect of the nonfunctional MotA-MotB(D33N) complex on wild-type motility. Motility of SJW1103 (wild-type) transformed with pTrc99AFF4 (V) or pNSK9(D33N) (MotA-MotB(D33N)) in semisolid agar plates at 30 °C.

Fig. S4. Effect of induction of MotA/MotB(D33N) in wild-type cells and MotA/MotB in *motA*/*motB* double null mutant on the rotation rate of the motor at high load. (*A*) Effect of steady-state induction of the nonfunctional MotA/MotB(D33N) complex. Histograms show the rotation rates of 1.0-μm beads attached to the sticky flagellar filaments of SJW46 (*fliC*(Δ204–292)) (upper) and those of the SJW46 cells transformed with pNSK9(D33N) grown with 10 mM (middle) or 25 mM IPTG (lower). Vertical dashed lines indicate rotation rates of 8 Hz and its multiples. The positional data of each bead were sampled at 1 kHz for 10 sec and the rotation rates were determined from power spectra using 1 sec data windows (1,024 points) at every 0.1 sec shift over the entire 10 sec data. The speed resolution was about 1 Hz. The number of cells measured for upper, middle, and lower were 22, 28, and 22, respectively. (*B*) Resurrection trace of the flagellar motor of the *Salmonella motA* and *motB* double null mutant transformed with pYC20 encoding the wild-type *motA* and *motB*. The trace shows resurrection starting with 2 or 3 stators and going on to 4, 5, 6 stators with a unit speed increment of 7–8 Hz. Cells were grown in Tryptone broth with 1-μM L-arabinose for 4 h at 30 °C. Measurement of the rotation rate of the 1.0-μm bead attached to the sticky flagellar filaments was begun 10 min after addition of 5 mM L-arabinose.
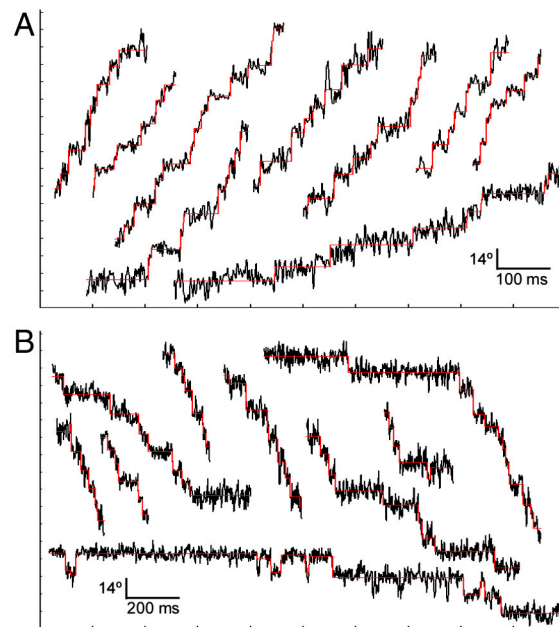
Fig. S5. Examples of stepping rotations detected in the motors of two different cells. (*A*) MM3076iC, and (*B*) SJW46. In both cases cells were grown with 25 μM IPTG for 4 h, and 100 nm-fluorescent beads were attached to the flagellar filaments. The bead images were recorded by the EMCCD camera at 0.4 msec intervals, with epifluorescence excitations using a dye laser (≈20 mW). All the measurements were carried out at an external pH 6.0 in the presence of 20 mM potassium benzoate at 23 °C. Red lines are steps determined by a step-finding algorithm.